Progress In Electromagnetics Research C, Vol. 48, 95–102, 2014

Novel Jamming Suppression Method Using Polarization SAR Data

Xiao-Hong Lin*, Guo-Yi Xue, and Pei-Guo Liu

Abstract—Barrage and deceptive jamming can mask the synthetic aperture radar (SAR) signals and render SAR useless. In this paper, a novel jamming suppression method based on polarization SAR (PolSAR) is proposed. After range compression, the barrage jamming has a noise-like characteristic while the real echo and deceptive jamming are focused. According to this, the barrage jamming is removed via a minimum entropy algorithm. Based on the different polarization characteristics between deceptive jamming and the real echo, the deceptive jamming can be suppressed by phase compensation in doppler domain. Simulation results are shown to demonstrate the validity of the proposed method.

1. INTRODUCTION

During the past fifty years, synthetic aperture radar (SAR) has become an important tool for information acquisition and been widely utilized in various fields [1]. On the other hand, there exist many kinds of jamming which may prominently worsen the imaging performance of SAR. Therefore, SAR should embed the ability to suppress multiple jamming at the same time. According to the working modes, SAR jamming can be classified into two types, i.e., barrage jamming and deceptive jamming [2]. Using strong noiselike signals, the barrage jamming prevents SAR from producing clear images. By retransmitting or simulating the true radar echo, the deceptive jamming can generate false targets in SAR image with small transmit power.

The traditional jamming suppression methods are based on the different characteristics of the jamming and real echo in time-frequency or space domain. Pulse diversity technologies are now widely applied to counter digital radio frequency memory (DRFM) jamming [3], yet they are incapable of suppressing the barrage jamming in high power effectively. Besides, many researchers have performed detailed studies on narrow-band interference suppression [4–6], which are unsuitable for removing

Received 24 January 2014, Accepted 8 March 2014, Scheduled 14 March 2014

* Corresponding author: Xiao-Hong Lin (linxiaohong2011@yeah.net).

The authors are with the School of Electronic Science and Engineering, National University of Defense Technology, China.

wide-band jamming. Space time adaptive processing (STAP) techniques are effective against noise jamming [7], while their effectiveness may reduce against deceptive jamming. In addition, digital beamforming can suppress both types of jamming by space-variant null steering [8]. However, many spatial degrees of freedom (DOF) may be required to attain full rejection whilst maintaining low sidelobes.

With the development of radar polarization techniques, polarimetric SAR (PolSAR) has been widely applied to target recognition and classification [9]. However, there are few papers to research its jamming suppression performance. Since different SAR systems may work in different polarizations, the jamming systems should comprise an operational capability against SAR of varying polarization characteristic. Considering the complexity of the equipment necessary to counter radar quasi-instantaneously, jamming devices utilize a simple type of polarized transmission such as slant-linear, circular, or more usually, elliptical. Hence, the jamming signal does not possess the same polarization characteristic as that of the echo from the illuminated targets which in general show large variations of the complex reflection coefficient, and this knowledge can be used to suppress jamming. Reference [10] first proposes an active-decoys jamming suppression method; however, it is unable to remove barrage jamming. [11, 12] make use of two key techniques in SAR domain — multichannel SAR and PolSAR to suppress both barrage and deceptive jamming; however, such methods require a complex hardware configuration and large calculated amount.

In this paper, a novel jamming suppression method for PolSAR is proposed to remove both barrage and deceptive jamming. In Section 2, the echo signal and jamming models are analyzed. Section 3 proposes a method to remove barrage jamming based on a minimum entropy algorithm. In Section 4, the deceptive jamming is removed via phase compensation. In Section 6, simulations are presented to verify the effectiveness of our algorithm.

2. POLSAR SIGNAL MODELS IN PRESENCE OF JAMMING

In this paper, we consider a stripmap PolSAR system works in time division polarization measurement scheme. The orthogonal antennas alternatively transmit horizontal (H) polarization and vertical (V) polarization pulses and receive the scattered echo at the same time. At the slow time t_{m1}, SAR transmits an H polarized pulse. Then, the horizontal-horizontal (HH) and horizontal-vertical (VH) polarization electromagnetic wave can be obtained. At the slow time t_{m2} ($t_{m2} = t_{m1} + T_a$), SAR transmits a V polarization signal, and then the vertical-horizontal (HV) and vertical-vertical (VV) polarization echoes can be received. Here, T_a denotes the pulse repetition interval (PRI).

Assume that SAR transmits a linear frequency modulation (LFM) pulses represented as $p(\tau)$ where τ denotes the fast time. For the ith point target in the illuminated scene, the scattered echoes in every polarization channel can be written as follows

$$\begin{cases} v_{iHH}(\tau, t_{m1}) = S_{iHH} p\left(\tau - \dfrac{2R_i(t_{m1})}{c}\right) \exp\left(-j4\pi \dfrac{R_i(t_{m1})}{\lambda}\right) \\ v_{iVH}(\tau, t_{m1}) = S_{iVH} p\left(\tau - \dfrac{2R_i(t_{m1})}{c}\right) \exp\left(-j4\pi \dfrac{R_i(t_{m1})}{\lambda}\right) \\ v_{iHV}(\tau, t_{m2}) = S_{iHV} p\left(\tau - \dfrac{2R_i(t_{m2})}{c}\right) \exp\left(-j4\pi \dfrac{R_i(t_{m2})}{\lambda}\right) \\ v_{iVV}(\tau, t_{m2}) = S_{iVV} p\left(\tau - \dfrac{2R_i(t_{m2})}{c}\right) \exp\left(-j4\pi \dfrac{R_i(t_{m2})}{\lambda}\right) \end{cases}, \tag{1}$$

where R_i is the range from the antenna to the point target, c the velocity of light, λ carrier wavelength, $\mathbf{S}_i = \begin{bmatrix} S_{iHH} & S_{iHV} \\ S_{iVH} & S_{iVV} \end{bmatrix}$ the scattering matrix of the target, and the matrix elements are scattering coefficients in HH, HV, VH, and VV polarization, respectively.

Suppose that there exist a barrage jammer transmitting the signal $p_b(\tau, t_m)$ and a deceptive jammer transmitting the signal $p_d(\tau, t_m)$. Ignoring the propagation effect of the electromagnetic, the complete

signals received by the receiver can be expressed as follows

$$\begin{cases} e_{HH}(\tau, t_{m1}) = \sum_i v_{iHH}(\tau, t_{m1}) + Jb_{HH}(\tau, t_{m1}) + Jd_{HH}(\tau, t_{m1}) \\ e_{VH}(\tau, t_{m1}) = \sum_i v_{iVH}(\tau, t_{m1}) + Jb_{VH}(\tau, t_{m1}) + Jd_{VH}(\tau, t_{m1}) \\ e_{HV}(\tau, t_{m2}) = \sum_i v_{iHV}(\tau, t_{m2}) + Jb_{HV}(\tau, t_{m2}) + Jd_{HV}(\tau, t_{m2}) \\ e_{VV}(\tau, t_{m2}) = \sum_i v_{iVV}(\tau, t_{m2}) + Jb_{VV}(\tau, t_{m2}) + Jd_{VV}(\tau, t_{m2}) \end{cases}, \tag{2}$$

where

$$\begin{cases} Jb_{HH}(\tau, t_{m1}) = h_{bH}(t_{m1}) p_b\left(\tau - \dfrac{R_b(t_{m1})}{c}, t_{m1}\right) \\ Jb_{VH}(\tau, t_{m1}) = h_{bV}(t_{m1}) p_b\left(\tau - \dfrac{R_b(t_{m1})}{c}, t_{m1}\right) \\ Jd_{HH}(\tau, t_{m1}) = h_{dH}(t_{m1}) p_d\left(\tau - \dfrac{R_d(t_{m1})}{c}, t_{m1}\right) \\ Jd_{VH}(\tau, t_{m1}) = h_{dV}(t_{m1}) p_d\left(\tau - \dfrac{R_d(t_{m1})}{c}, t_{m1}\right) \\ Jb_{HV}(\tau, t_{m2}) = h_{bH}(t_{m2}) p_b\left(\tau - \dfrac{R_b(t_{m2})}{c}, t_{m2}\right) \\ Jb_{VV}(\tau, t_{m2}) = h_{bV}(t_{m2}) p_b\left(\tau - \dfrac{R_b(t_{m2})}{c}, t_{m2}\right) \\ Jd_{HV}(\tau, t_{m2}) = h_{dH}(t_{m2}) p_d\left(\tau - \dfrac{R_d(t_{m2})}{c}, t_{m2}\right) \\ Jd_{VV}(\tau, t_{m2}) = h_{dV}(t_{m2}) p_d\left(\tau - \dfrac{R_d(t_{m2})}{c}, t_{m2}\right) \end{cases}. \tag{3}$$

R_b is the distance between SAR and the barrage jammer, while R_d denotes the range from SAR to the deceptive jammer. $\mathbf{h}_b(t_m) = [h_{bH}(t_m), h_{bV}(t_m)]^T$ and $\mathbf{h}_d(t_m) = [h_{dH}(t_m), h_{dV}(t_m)]^T$ are the Jones vectors of the barrage and deceptive jamming, respectively. Here, $h_{bV}(t_m) = \rho_b h_{bH}(t_m)$ where $\rho_b = \tan(\gamma_b)\exp(j\delta_b)$ is the polarization ratio, $\gamma_b \in [0, \pi/2]$ and $\delta_b \in (0, 2\pi]$. For example, $\gamma_b = \pi/4$ and $\delta_b = \pi/2$ in the left-circular polarization. Similarly, $h_{dV}(t_m) = \rho_d h_{dH}(t_m)$ where $\rho_d = \tan(\gamma_d)\exp(j\delta_d)$.

3. BARRAGE JAMMING SUPPRESSION

The barrage jamming is non-coherent to SAR transmitted signal while the deceptive jamming and scattered echo are coherent. After the range compression operation, the barrage jamming has a noise-like characteristic, and its energy will be distributed uniformly in the range direction. On the contrary, the deceptive jamming and target echo will be focused. In the field based on information theory, entropy is a statistic measure of randomness, disorder, or more precisely unpredictability. That is to say, the barrage jamming will bring about large entropy in the range-compressed domain. Next, we will propose a minimum entropy algorithm to remove the barrage jamming.

In our algorithm, we firstly perform range compression on (2), and the signals can be expressed as e'_{HH}, e'_{VH}, e'_{HV} and e'_{VV}. Then, we construct a entropy function as follows

$$f_{b1}(\gamma, \delta) = -\sum_{q=1}^{Q} |\hat{e}_1(q, t_{m1})| \ln(|\hat{e}_1(q, t_{m1})|), \tag{4}$$

where Q is the fast time sample number, $\hat{e}_1(q,t_{m1}) = |\hat{e}_{b1}(q,t_{m1})|^2 / \sum_{q=1}^{Q} |\hat{e}_{b1}(q,t_{m1})|^2$, $\hat{e}_{b1}(q,t_{m1}) = e'_{VH}(q,t_{m1}) - \tan(\gamma)\exp(j\delta)e'_{HH}(q,t_{m1})$. As mentioned above, the residual barrage jamming in $\hat{e}_{b1}(q,t_{m1})$ will cause more disorder. When $\gamma = \gamma_b$ and $\delta = \delta_b$, the barrage jamming will be removed completely, and the entropy f_{b1} will become minimum. According to this view, the estimated values of γ_b and δ_b can be obtained as

$$(\hat{\gamma}_b, \hat{\delta}_b) = \min_{\gamma,\delta} f_{b1}(\gamma,\delta). \tag{5}$$

Now, the (γ_b, δ_b) estimation is formulated as a nonlinear optimization problem. This problem is difficult to solve using traditional search techniques because of its non-convex nature, resulting in multiple local minima. Particle swarm optimization (PSO) is a population-based and stochastic optimization technique. Compared to conventional optimization techniques such as genetic algorithm, PSO takes advantage of its algorithm simplicity and robustness. In this paper, we utilize PSO algorithm to search for the optimum solution.

In our PSO algorithm, Formula (5) is used as the fitness function. All the encountered positions (γ, δ) of the particles are evaluated by this fitness function to represent how well the particles satisfy the parameters. The implementation steps of PSO algorithm can be found in [13]. In order to obtain higher estimation accuracy, we perform the (γ, δ) estimation at several slow times, and the mean of estimated values will become the final result.

With the estimated value $\hat{\rho}_b = \tan(\hat{\gamma}_b)\exp(j\hat{\delta}_b)$, the barrage jamming of the VH and HH polarization channels can be suppressed, and the new signal becomes

$$\hat{e}_{b1}(\tau,t_{m1}) = e'_{VH}(\tau,t_{m1}) - \hat{\rho}_b e'_{HH}(\tau,t_{m1}). \tag{6}$$

In the same way, we can obtain the barrage-jamming-removed signal at the slow time t_{m2}, which is written as

$$\hat{e}_{b2}(\tau,t_{m2}) = e'_{VV}(\tau,t_{m2}) - \hat{\rho}_b e'_{HV}(\tau,t_{m2}), \tag{7}$$

where e'_{VV} and e'_{HV} are the digital signals in the VV and HV polarization channels after range compression respectively.

4. DECEPTIVE JAMMING SUPPRESSION

Over a very short time (T_a is usually less than 1 millisecond), the polarization of the deceptive jamming can be approximated to be invariable, that is

$$\mathbf{h}_d(t_{m2}) \approx \mathbf{h}_d(t_{m1}). \tag{8}$$

The polarization scattering property of the real target changes very little, and its scattering coefficients satisfy the reciprocity theorem

$$S_{iVH} = S_{iHV}. \tag{9}$$

From (8) and (9), the relationship between the received signals in different polarization channels can be obtained. For the deceptive jamming,

$$JD_{HV}(f_a) = JD_{HH}(f_a)\exp(j2\pi f_a T_a), \tag{10}$$

$$JD_{VV}(f_a) = JD_{VH}(f_a)\exp(j2\pi f_a T_a), \tag{11}$$

where JD_{HH}, JD_{HV}, JD_{VH} and JD_{VV} are the doppler spectrums of the deceptive jamming after range compression and range cell migration correction (RCMC); f_a denotes the doppler frequency. For the real target,

$$V_{iHV}(f_a) = V_{iVH}(f_a)\exp(j2\pi f_a T_a), \tag{12}$$

where V_{iHV} and V_{iVH} represent the doppler spectrums of the ith target echo after range compression and RCMC.

In our jamming suppression technique, we also perform RCMC on (6) and (7), and transform these signals into doppler domain. According to (2), (3), (6) and (7), the transformed signals can be expressed as follows

$$\hat{E}_{b1}(\tau, f_a) = \sum_i \left(V_{iVH}(\tau, f_a) - \hat{\rho}_b V_{iHH}(\tau, f_a)\right) + JD_{VH}(\tau, f_a) - \hat{\rho}_b JD_{HH}(\tau, f_a), \tag{13}$$

$$\hat{E}_{b2}(\tau, f_a) = \sum_i \left(V_{iVV}(\tau, f_a) - \hat{\rho}_b V_{iHV}(\tau, f_a)\right) + JD_{VV}(\tau, f_a) - \hat{\rho}_b JD_{HV}(\tau, f_a). \tag{14}$$

It can be seen that the deceptive jamming in $\hat{E}_{b1}(\tau, f_a)$ is differentiated from that in $\hat{E}_{b2}(\tau, f_a)$ with a phase term $\exp(j2\pi f_a T_a)$. Thus, we can remove the deceptive jamming, through the following phase compensation,

$$V(\tau, f_a) = \hat{E}_{b2}(\tau, f_a) - \hat{E}_{b1}(\tau, f_a) \exp(j2\pi f_a T_a). \tag{15}$$

Finally, the jamming-removed image can be obtained via the conventional azimuth compression. The whole flow chart of our technique is shown as Figure 1.

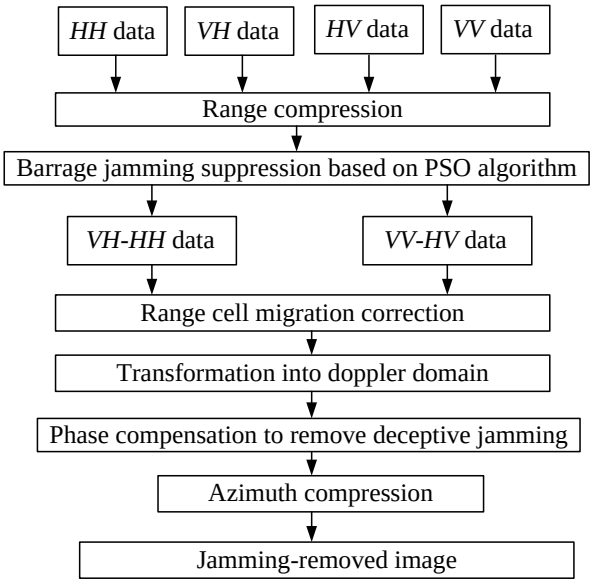

Figure 1. Flow chart of the proposed technique.

5. THE IMAGING RESULTS OF REAL TARGETS AFTER JAMMING SUPPRESSION

According to the formulas (9)∼(15), we have

$$\begin{aligned} V(\tau, f_a) &= \sum_i \left(V_{iVV}(\tau, f_a) - \hat{\rho}_b V_{iHV}(\tau, f_a)\right) - \beta(f_a) \sum_i \left(V_{iVH}(\tau, f_a) - \hat{\rho}_b V_{iHH}(\tau, f_a)\right) \\ &= \sum_i V_{iVV}(\tau, f_a) + \hat{\rho}_b \sum_i \beta(f_a) V_{iHH}(\tau, f_a) - (\hat{\rho}_b + 1) \sum_i \beta(f_a) V_{iVH}(\tau, f_a), \end{aligned} \tag{16}$$

where $\beta(f_a) = \exp(j2\pi f_a T_a)$. After performing inverse fast Fourier transform (IFFT) in the doppler domain, the useful signal can be obtained as follow

$$\begin{aligned} v(\tau, t_m) &= \sum_i v_{iVV}(\tau, t_{m2}) + \hat{\rho}_b \sum_i v_{iHH}(\tau, t_{m1} + T_a) - (\hat{\rho}_b + 1) \sum_i v_{iVH}(\tau, t_{m1} + T_a) \\ &= \sum_i v_{iVV}(\tau, t_{m2}) + \hat{\rho}_b \sum_i v_{iHH}(\tau, t_{m2}) - (\hat{\rho}_b + 1) \sum_i v_{iVH}(\tau, t_{m2}). \end{aligned} \tag{17}$$

It can be seen that the useful signal is a simple linear superposition of the real VV, HH and VH polarization echoes received at the slow time t_{m2}, equivalently.

The imaging result by using the range Doppler algorithm (RDA) [14] can be derived as

$$I(\tau, t_m) = \sum_i [S_{iVV} + \hat{\rho}_b S_{iHH} - (\hat{\rho}_b + 1) S_{iVH}] \times A_0 \text{sinc}\left(B\left(\tau - \frac{2R_{i0}}{c}\right)\right) \text{sinc}\left(B_d\left(t_{m2} - \frac{x_i}{v}\right)\right) \exp\left(-j\frac{4\pi R_{i0}}{\lambda}\right), \quad (18)$$

where A_0 is a constant, B the signal bandwidth, B_d the Doppler bandwidth, v the radar velocity along the azimuth direction, and R_{i0} and x_i denote respectively the nearest slant range and the azimuth coordinate of the ith point target.

Without jamming, the PolSAR can provide HH, VV, VH and HV polarization images. These polarimetric measurements will help to refine tomographic results. From (18), only one image can be obtained after removing the jammings with our method. That is to say, jamming suppression also brings about some loss of polarimetric information. In addition, the amplitude of the ith imaging point is proportional to $\psi_i = |S_{iVV} + \hat{\rho}_b S_{iHH} - (\hat{\rho}_b + 1) S_{iVH}|$. if $\psi_i = 0$, then the imaging point is also eliminated. For a high resolution radar, a target usually posses an asymmetrical shape and is constructed by various types of strong scattering centers, whose scattering matrixes depend on their shapes and conducting properties of a small surface around them [15]. That is to say, for the target, there exist few scattering centers whose scattering coefficients fit $\psi_i = 0$, and it will not significantly affect the performance of target recognition.

6. SIMULATION AND ANALYSIS

In order to evaluate the effectiveness of the presented method, some numerical simulation results are provided in this section. The SAR system parameters are set as follows: the carrier frequency $f_c = 2\,\text{GHz}$, the bandwidth $B = 40\,\text{MHz}$ and the pulse repetition frequency (PRF) $f_p = 640\,\text{Hz}$.

In this simulation, the SAR works at stripmap mode, and the resolution is $3.75 \times 2\,\text{m}$. The real scene includes two rows of tank parked in the meadow, and each row contains 26 tanks with an interval of 4 m between the adjacent tanks. For simplicity, these tanks are modeled as the dihedral corner reflectors whose normalized scattering matrixes are all $\begin{bmatrix} -1 & 0 \\ 0 & 1 \end{bmatrix}$, and the polarimetric covariance matrix of the meadow clutter is set as $\begin{bmatrix} -1 & 0 & 0.53 \\ 0 & 0.19 & 0 \\ 0.53 & 0 & 1.03 \end{bmatrix}$. In addition, there exist a barrage jammer and a deceptive jammer. The barrage jammer transmits random noise signal with the signal-to-jamming ratio (SJR) $-55\,\text{dB}$ in the right-hand circular polarization, while the other jammer transmits a forest-scene deceptive jamming with the SJR $-10\,\text{dB}$ in the left-hand circular polarization.

Figure 2 shows the imaging results of the contaminated echoes in different polarization channels. It can be seen that the tank targets are smeared, and SAR is unable to perform accurate target detection. First, based on the minimum algorithm, we perform the ρ_b estimation at 10 randomly selected slow times. The mean of these estimated values is $\hat{\rho}_b = -0.0026 - 0.9996 \times i$. Now, the barrage jamming can be removed according to (6) and (7). Figure 3 shows the imaging results after barrage jamming suppression using the data received by different polarization channels. Note that the tank targets are still buried by a deceptive forest scene.

We perform RCMC operation on the barrage-jamming-removed signals and transform them into range-doppler domain. Then, the deceptive jamming can be eliminated based on (15). The final imaging result is shown in Figure 4. It can be observed that the barrage and deceptive jamming have been suppressed effectively, and the tank targets are focused well. However, since we utilize the channel cancelation method to remove the two jamming, only one SAR image can be obtained finally. That is to say, the jamming suppression also brings about some loss of the target information for PolSAR.

7. CONCLUSION

Image degradation due to various jamming is an important problem in SAR imaging, which cannot be neglected during SAR image analysis. At present, many methods are proposed to remove jamming in time-frequency or space domain. However, they may cease to be effective when the jamming works in wide-band or the jammer locates inside the main lobe region. Fortunately, there exists a distinct polarization character between the illuminated target and the jammer. Based on this idea, a new jamming suppression method is proposed in this paper. First, after range compress, the barrage jamming can be removed with a minimum entropy algorithm. Then, the deceptive jamming can be suppressed in range-doppler domain via phase compensation. The simulation results show that our method can suppress the barrage and deceptive jamming effectively. However, our method will bring about some loss of the target information for PolSAR.

REFERENCES

1. Yang, W., J. Chen, H. Zeng, J. Zhou, P. Wang, and C. S. Li, "A novel three-step image formation scheme for unified focusing on spaceborne SAR data," *Progress In Electromagnetics Research*, Vol. 137, 621–642, 2013.
2. Zhou, F., G. Sun, X. Bai, and Z. Bao, "A novel method for adaptive SAR barrage jamming suppression," *IEEE Geoscience and Remote Sensing Letters*, Vol. 9, No. 2, 292–296, 2012.
3. Soumekh, M., "SAR-ECCM using phase-perturbed LFM chirp signals and DRFM repeat jammer penalization," *IEEE Transactions on Aerospace and Electronic Systems*, Vol. 42, No. 1, 191–205, 2006.
4. Kimura, H., T. Nakamura, and K. P. Papathanassiou, "Suppression of ground radar interference in JERS-1 SAR data," *IEICE Transaction on Communication*, Vol. E87B, 3759–3765, 2004.
5. Lu, G., B. Tang, and G. Gui, "Deception ECM signals cancellation processor with joint time-frequency pulse diversity," *IEICE Electronics Express*, Vol. 8, 1608–1613, 2011.
6. Feng, J., H. Zheng, Y. Deng, and D. Gao, "Application of subband spectral cancellation for SAR narrow-band interference suppression," *IEEE Geoscience and Remote Sensing Letters*, Vol. 9, No. 2, 190–193, 2012.
7. Rosenberg, L. and D. Gray, "Anti-jamming techniques for multichannel SAR imaging," *IEE Proceedings: Radar, Sonar and Navigation*, Vol. 153, No. 3, 234–242, 2006.
8. Paine, A. S., "An adaptive beamforming technique for countering synthetic aperture radar (SAR) jamming threats," *IEEE 2007 Radar Conference*, 630–634, 2007.

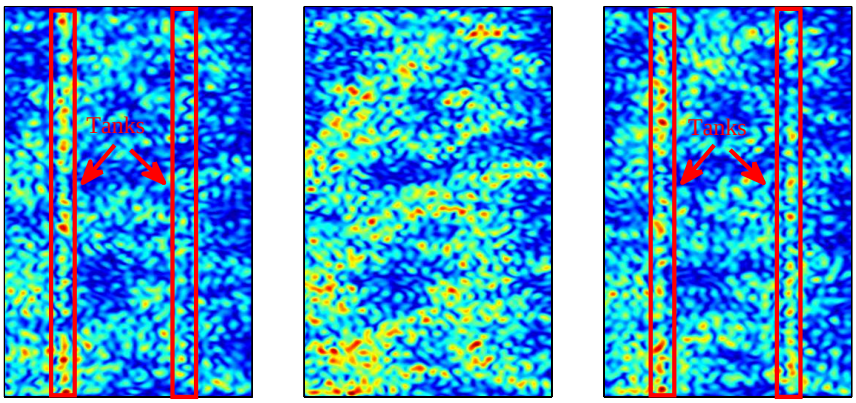

Figure 2. The imaging results before jamming suppression. (a) HH channel. (b) HV channel. (c) VV channel.

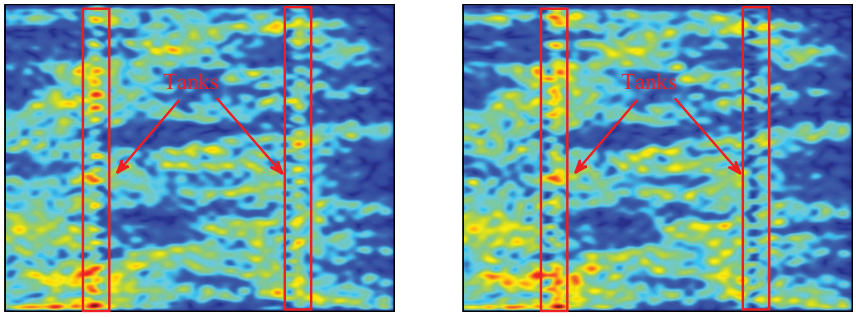

(a) (b)

Figure 3. The imaging results before barrage jamming suppression. (a) Using the data received by VH and HH channel. (b) Using the data received by VV and HV channel.

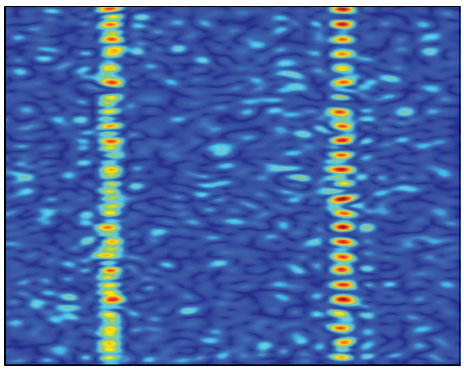

Figure 4. The imaging result after barrage and deceptive jamming suppression.

9. Brekke, C. and S. N. Anfinsen, "Ship detection in ice-infested waters based on dual-polarization SAR imagery," *IEEE Geoscience and Remote Sensing Letters*, Vol. 8, No. 3, 391–395, 2011.
10. Dai, D. H., X. S. Wang, S. P. Xiao, and Y. Z. Li, "Discrimination and suppression of active-decoys jamming in PolSAR," *Acta Electronica Sinica*, Vol. 9, 1779–1783, 2007.
11. Guo, R., G. C. Sun, F. Zhou, and M. D. Xing, "Jamming suppression in D-PolSAR System," *Journal of Electronics and Information Technology*, Vol. 32, 1343–1349, 2010.
12. Guo, R., G. C. Sun, Y. Wang, F. Zhou, and M. D. Xing, "Analysis of the active jamming suppression in polarimetric SAR," *Journal of Astronautics*, Vol. 32, 1365–1372, 2011.
13. Lim, T. S., V. C. Koo, H. T. Ewe, and H. T. Chuah, "A SAR autofocus algorithm based on particle swarm optimization," *Progress In Electromagnetics Research B*, Vol. 1, 159–176, 2008.
14. Wei, S. and Z. H. Fang, "Research on estimation of the Doppler centroid by Matlab," *Chinese Journal of Ship Research*, Vol. 3, No. 03, 51–55, 2004.
15. Giuli, D., "Polarization diversity in radars," *Proceedings of the IEEE*, Vol. 74, No. 2, 245–269, 1986.